## Title

Near-IR transillumination and reflectance imaging at 1,300 nm and 1,500—1,700 nm for in vivo caries detection



## Journal

Lasers in Surgery and Medicine, 48(9)

## ISSN

0196-8092

## Authors

Simon, Jacob C
Lucas, Seth A
Staninec, Michal
et al.

## Publication Date

2016-11-01

## DOI

10.1002/lsm.22549

Peer reviewed

HHS Public Access

Author manuscript

*Lasers Surg Med*. Author manuscript; available in PMC 2017 July 03.

Published in final edited form as:

*Lasers Surg Med*. 2016 November ; 48(9): 828–836. doi:10.1002/lsm.22549.

# Near-IR Transillumination and Reflectance Imaging at 1,300 nm and 1,500–1,700nm for In Vivo Caries Detection

**Jacob C Simon**, **Seth A. Lucas, DDS**, **Michal Staninec, DDS, phD**, **Henry Tom**, **Kenneth H. Chan**, **Cynthia L. Darling, phD**, **Matthew J. Cozin, DDS**, **Robert C. Lee, DDS, phD**, and **Daniel Fried, phD***

University of California, San Francisco, San Francisco 94143-0758 California

## Abstract

**Introduction—**Several studies suggest that near-IR imaging methods at wavelengths longer than 1,300nm have great potential for caries detection. In this study, the diagnostic performance of both near-IR transillumination and near-IR reflectance was assessed on teeth scheduled for extraction due to orthodontic treatment ($n$ = 109 teeth on 40 test subjects).

**Methods—**Three intra-oral near-IR imaging probes were fabricated for the acquisition of *in vivo* images using a high definition InGaAs camera and near-IR broadband light sources. Two transillumination probes provided occlusal and approximal images using 1,300nm light which manifests the highest transparency in enamel. A third reflectance probe utilized cross-polarization and operated at wavelengths greater than 1,500nm where water absorption is higher which reduces the reflectivity of sound tissues, significantly increasing lesion contrast. Teeth were collected after extraction and sectioned and examined with polarized light microscopy and microradiography which served as the gold standard. In addition, radiographs were taken of the teeth and the diagnostic performance of near-IR imaging was compared with radiography.

**Results—**Near-IR imaging was significantly more sensitive ($P < 0.05$) than radiography for the detection of lesions on both occlusal and proximal surfaces.

**Conclusion—**Near-IR imaging methods are ideally suited for screening all tooth surfaces for carious lesions.

### Keywords

caries detection; near-IR imaging; transillumination; reflectance

## Introduction

Dental enamel manifests its highest transparency near 1,300nm where the scattering coefficient of enamel is 20–30 times lower than it is at visible wavelengths [1,2]. Due to the high transparency, novel imaging configurations are feasible in which the tooth can be

*Correspondence to: Daniel Fried, Department of Preventive and Restorative Dental Sciences, University of California, San Francisco, 707 Parnassus Avenue, San Francisco, CA 94143. daniel.fried@ucsf.edu.

Conflict of Interest Disclosures: All authors have completed and submitted the ICMJE Form for Disclosure of Potential Conflicts of Interest and none were reported.

imaged from the occlusal surface after shining light at and below the gum line, which we call occlusal transillumination [3,4]. Upon demineralization the scattering coefficient of enamel increases by 1–2 orders of magnitude at 1,300nm to yield high contrast between sound and demineralized enamel for caries detection [5]. Therefore, this wavelength range is ideally suited for the transillumination of approximal dental caries lesions (dental decay in between teeth). Previous studies carried out by our group over the past 12 years have demonstrated that approximal lesions can be imaged by occlusal transillumination of the proximal contact points between teeth and by directing near-IR light below the crown while imaging the occlusal surface [4,6,7]. The latter approach is capable of imaging occlusal lesions as well with high contrast [3,4,8–10]. Optical transillumination was used extensively before the discovery of X-rays for detection of dental carious lesions. Over the past two decades there has been continued interest in this method, especially with the availability of high intensity fiber optic based illumination systems for the detection of approximal lesions [11–16]. A digital fiber optic transillumination system, called DiFoti from Electro-optics Sciences (Irvington, NY) that utilizes visible light for the detection of caries lesions was introduced several years ago [17]. Carious lesions appear dark upon fiber optic transillumination (FOTI) due to increased scattering and absorption by the lesion reducing optical transmission. Several studies have been carried out using visible light transillumination either as an adjunct to bite-wing radiography or as a competing method for the detection of approximal carious lesions [17–20]. However, FOTI and DIFOTI operate in the visible range where strong light scattering prevents imaging through the entire tooth [1,2]. More recently, another system has been introduced called the Diagnocam from Kavo (Biberach, Germany) that uses an occlusal transillumination probe with 780 nm light [21,22]. We previously investigated using transillumination imaging at 830nm which has the advantage of utilizing a low-cost silicon CCD sensor optimized for the near-IR. The 830nm system was capable of higher performance than visible systems, but the contrast was significantly lower than 1,310nm and simulated lesions could not be imaged through the full enamel thickness [6]. Other groups have confirmed the high potential of the near-IR for imaging dental decay [23,24].

There are other important advantages of imaging dental decay in the near-IR. Stains that are common on tooth occlusal surfaces do not interfere at near-IR wavelengths since none of the known chromophores absorb light in the near-IR beyond 1,300nm [3,24]. More recently, Almaz et al. demonstrated that it was necessary to use near-IR wavelengths greater than 1,150nm to avoid significant interference from stains when measuring lesion contrast in reflectance and transillumination modalities [25]. Therefore, stains can be easily differentiated from actual demineralization in the near-IR range, which is not possible at visible wavelengths. Chung et al. [26] indicated that absorption due to stains contributed more to the lesion contrast than increased scattering due to demineralization at visible wavelengths [27]. Since it is impractical to remove stains from the deep grooves and fissures on tooth occlusal surfaces, lack of interference from stains at longer near-IR wavelengths is a significant advantage.

Additionally, reflectance imaging at wavelengths greater than 1,300nm have yielded extremely high contrast of early demineralization [24,26,28–31]. More recent near-IR imaging studies suggest that near-IR wavelengths coincident with high water absorption

namely, 1,450nm or 1,500–1,700nm, yield the highest contrast of demineralization on tooth surfaces. We hypothesize that higher water absorption at these wavelengths reduces the reflectivity in the underlying sound enamel and dentin resulting in even higher contrast between sound and demineralized enamel than observed at 1,300nm. Hyperspectral reflectance measurements by Zakian et al. [24] show that the tooth appears darker at wavelengths coincident with higher absorption by water.

Two prior clinical studies involving near-IR transillumination imaging have been published [4,32]. In 2009, we demonstrated that approximal lesions that appeared on radiographs could be detected with near-IR imaging with similar sensitivity [4]. This was the first step in demonstrating the clinical potential of near-IR imaging for approximal caries detection. Even though the sensitivity of radiographs is not very high [33–37], most studies indicate the specificity of radiographs is above 90%, which makes it a suitable standard for comparison with the first test of this new imaging technology. In addition to demonstrating that the sensitivity of near-IR transillumination was as high as radiography, we found that multiple imaging geometries could be employed to aid in diagnosis, and that the occlusal imaging geometry in which light is applied near the gumline is extremely valuable for detecting approximal lesions [4]. In a second study completed in 2011, teeth with non-cavitated occlusal caries lesions that were not radiopositive were examined in test subjects using near-IR occlusal transillumination at 1,300nm prior to restoration [32]. That study demonstrated that occlusal caries lesions can be imaged with high contrast *in vivo* and that near-IR occlusal transillumination is an excellent screening tool for occlusal lesions. The next logical step is to carry out *in vivo* studies in which the near-IR is used as a screening tool to detect lesions and assess the diagnostic performance of our custom fabricated near-IR system. In addition, the clinical potential of near-IR reflectance imaging has not been investigated.

In this study, we assessed the diagnostic performance of both near-IR transillumination and near-IR reflectance probes that we fabricated in our laboratory for both occlusal and approximal lesions. Premolar teeth scheduled for extraction due to orthodontic considerations were imaged and after extraction the teeth were collected and sectioned and examined with polarized light microscopy and transverse microradiography which served as the gold standard. In addition, extra-oral radiographs were taken of teeth and the diagnostic performance of near-IR imaging was compared with radiography.

## Materials and Methods

### Visible Images

A Dino-Lite digital microscope, Model AM7013MZT, AnMO Electronics Corp. (New Taipei City, Taiwan) equipped with a dental mirror was used to acquire visual images, both wet and dry, of the patients' teeth prior to near-IR imaging. The digital microscope captures 5 megapixel (2,592 × 1,944) color still images and video. Eight white LED lights contained in the camera illuminate the teeth and the device features a single polarizing element that helps reduce glare. Visual images are taken for reference and compared with near-IR techniques at the beginning of each imaging session.

### Near-IR Imaging System

The individual probes are designed to work interchangeably by attaching to a set of universal components connecting the probes to the near-IR camera through relay optics. Two near-IR achromatic lenses, $f$ = 60 mm AC254-060-C and $f$ = 150mm AC254-150-C (Thorlabs, Newton, NJ) were used to project the captured light onto a high sensitivity InGaAs focal plane array camera, Model GA1280J (Sensors Unlimited, Princeton, NK) with a 1,280 × 1,024 pixel format and 15 μm pixel pitch. A 360° rotation element allows simple rearrangement of the imaging probe to access the upper and lower teeth. The assembly is physically supported via an aluminum post attached to an elastic band wrapped around the forearm of the clinician. A power supply and output cable attaches to the backside of the camera and connects the instrumentation with computers and optical fibers through a mesh bundle. Near-IR video was acquired at a rate of 30 frames per second and the imaging time ranged from 1 to 2 minutes per probe.

### Near-IR Approximal Transillumination

Near-IR approximal transillumination produces diagnostic images similar in appearance to that of conventional bitewing X-rays from both the facial and lingual viewpoints. Figure 1A is a schematic drawing of the imaging probe that couples with the common optical components of the system described in Near-IR Imaging System section. Light centered at 1,310nm is generated using a super-luminescent laser diode (SLD), Model SLD72 (COVEGA Corporation, Jessup, MD) with 50nm bandwidth. Fiber optic cables are used to deliver the light into a Teflon diffusing element. Light emitted from the diffusing element propagates through the tooth, that is located between the diffusing element and a right-angled mirror and is reflected down the imaging tube through the relay optics and onto the focal plane array of the camera. Each tooth is imaged from the facial side and then the probe is rotated 180° and the tooth is imaged from the lingual position. The approximal transillumination probe delivered a 6–10 mW cone of light onto the lingual and buccal surfaces with a circular area of 1.5 cm in diameter.

### Near-IR Occlusal Transillumination

Near-IR occlusal transillumination produces diagnostic images unique to near-IR imaging systems and is capable of detecting both occlusal and approximal lesions. Figure 1B shows a diagram of the probe. Light centered at 1,310nm is generated using a SLD, SLD72 with a 50nm bandwidth. Fiber optic cables are used to deliver the light into two diffusing elements made of Teflon. The diffusing elements are positioned using copper tubes that direct the light below the cementum-enamel junction (CEJ) into the gingival tissue from both the lingual and facial sides at a shallow angle. Light that enters the tooth diffuses throughout its interior and out the occlusal tooth surface. A right-angled mirror reflects the emitted light down the imaging tube through the relay optics and onto the focal plane array of the camera. The probe is designed to rotate 180° for the imaging of both upper and lower teeth. The occlusal transillumination probe delivered a 6–10mW cone of light onto the lingual and buccal surfaces with a circular area 3mm in diameter.

### Cross-polarized Near-IR Reflectance

Initially, a near-IR reflectance probe without cross-polarization elements was used to acquire *in vivo* images. For this probe, light from an SLD operating at 1,600nm was used to deliver NIR light into a fiber optic with a Teflon diffusing element. Light passes through the hollow width of the imaging probe and interacts with the surface of the tooth where it is reflected or scattered back towards the relay right-angled mirror. Specular reflections from the tooth surfaces make identification of demineralized areas difficult. To overcome this phenomenon, cross-polarization techniques are used to reduce the amount of reflected light reaching the detector.

A schematic drawing of the cross-polarized reflectance probe is shown in Figure 1C. Light from a tungsten-halogen lamp, Model HL-2000 (Ocean Optics, Dunedin, Florida) and a long pass 1,500nm filter, Model FEL1500 (Thorlabs) was used. The tungsten-halogen source replaced the SLD source used by the previous model in order to reduce speckle noise from interference of the coherent light. Wavelengths longer than 1,500nm were delivered to the probe through a glass fiber optic waveguide (Dolan-Jenner, Boxborough, MA). The light emitted from the waveguide is incident on a polarizing beam splitter cube, Model PBS054 (Thorlabs) where a single linear polarization state is reflected down through the hollow width of the probe and onto the sample surface. The light interacts with the tooth and is reflected or scattered back to a right-angled mirror and directed down the imaging tube to the focal plane array. A second linear polarizer, Model MPIRE-100-C (Thorlabs) inserted into the rotating element and oriented orthogonally to the polarization state of the first is used to eliminate specular reflected light from reaching the detector. The reflectance probe delivered a 6–10 mW cone of light over a circular area 1.5cm in diameter.

### Patient Recruitment

After obtaining IRB approval and written informed consent, 40 participants were recruited from the patient population of the University of California, San Francisco School of Dentistry. Subjects aged 12–60 with 2–4 premolars (universal numbering system 4/5, 12/13, 20/21, and 28/29) scheduled for extraction were recruited. A total of 109 teeth were imaged in the study. None of the collected premolars were excluded from the study.

### Visible and Near-IR Clinical Imaging Protocol

Each premolar tooth was imaged *in vivo* with the visible and near-IR imaging systems while viewing a live video feed of the captured images on a computer monitor. Imaging was employed in the following order: (i) Conventional photos of the teeth were taken (both wet and air dried) using a digital camera; (ii) Cross-polarized near-IR reflectance images were acquired for the detection of surface demineralization in the pits and fissures and other external (surface) signs of decay; (iii) Occlusal near-IR transillumination was used to detect approximal lesions and deeper (more severe) occlusal lesions; (iv) Approximal near-IR transillumination images were captured for the detection of lesions on proximal surfaces. During near-IR reflectance imaging an air spray was employed to dry the tooth surface (increasing lesion contrast) and prevent water/saliva accumulation on the occlusal surface. The air spray is also used to remove air bubbles during near-IR transillumination imaging.

The video output from the InGaAs array was recorded and displayed simultaneously for all three near-IR probes through the coupled computer system.

### Extra-Oral Digital Radiographs

After the extracted premolars ($n$ = 109) were collected from the clinic, samples were sterilized using gamma radiation and stored in 0.1% thymol solution to maintain tissue hydration and prevent bacterial growth. Then, samples were mounted in black orthodontic acrylic blocks (Great Lakes Orthodontics, Tonawanda, NY) and imaged with digital radiographs using a CareStream 2200 System (Kodak, Rochester, NY) operating at 60 kV.

### Clinical Evaluation of Digital Radiographs and Near-IR Images

One clinician examined only the diagnostic radiographs while another clinician examined only the near-IR digital videos for each of the near-IR probes while blinded to the other modalities. Each clinician was a practicing dentist with an active private practice and more than 20 years of experience. The clinician chosen to evaluate digital radiographs was a trained dental educator. The clinician who performed near-IR inspection had prior experience with near-IR transillumination and had participated in our previous near-IR transillumination study [4].

During video recording the probes were rotated to acquire images at various angles. This was particularly important for near-IR reflectance imaging to avoid the interference of specular reflection from the tooth. Specular reflection is only visible at normal incidence and vanishes at other angles while lesions remain visible at all angles. Based on the diagnostic video, evaluators diagnosed the presence and depth (S, E1, E2, D1, D2) of approximal and occlusal lesions: S—sound (no lesion present); E1—lesion present with depth restricted to the outer half of enamel; E2—lesion present with depth greater than half the enamel thickness but not yet penetrating into the dentin; D1—lesion present and penetrating into the inner half of dentin; D2—lesion present and penetrating into second half of dentin. Differential diagnosis was requested to ensure that the clinicians would not overlook the earliest signs of decay in each modality. The comparison of the NIR and X-ray did not account for the differential diagnosis of lesion depth.

### Sectioning, Polarized Light Microscopy (PLM), and Transverse Microradiography (TMR)

After all diagnostic images were captured, samples were serially sectioned into ~200 μm thick mesio-distal slices using a linear precision saw, Isomet 5000 (Buehler, Lake Buff, IL). Thin sections were subjected to histological examination by polarized light microscopy and transverse microradiography.

Polarized light microscopy (PLM) was used for histological examination using a Meiji Techno RZT microscope (Saitama, Japan) with an integrated digital camera, Canon EOS Digital Rebel XT (Tokyo, Japan). Sample sections 200 μm thick were imbibed in deionized water and examined in the bright field mode with crossed-polarizers and a red I plate (550 nm retardation).

A custom-built digital TMR system was used to measure mineral loss in the lesion areas. A high-speed motion control system with UTM150 and 850G stages and an ESP300 controller Newport (Irvine, CA) coupled to a video microscopy and laser targeting system was used for precise positioning of the tooth samples in the field of view of the imaging system. The volume percent mineral for each thin section was determined by comparison with a calibration curve of X-ray intensity versus sample thickness created using sound enamel sections of 86.3 ± 1.9 vol.% mineral varying from 50 to 300 μm in thickness using IgorPRO image analysis software. The calibration curve was validated via comparison with cross-sectional microhard-ness measurements, $r^2 = 0.99$ [38]. Image line profiles 100–150 pixels in width were extracted from the sample ROI representing the percent mineral at each pixel.

TMR images for occlusal and proximal surfaces of each sample were ranked based on lesion depth using the following ordinal ratings (S, E1, E2, D1, D2) as defined in Evaluation of Digital Radiographs and Near-IR Images section.

### Statistical Analysis

The depths of carious lesions located on the occlusal and proximal surfaces measured from histological TMR analysis were analyzed using the $\chi^2$ statistic calculated using InStat software (GraphPad, San Diego, CA). The diagnostic performance of each modality was measured by comparing the clinical evaluations of digital X-rays and NIR images to the gold standard TMR measurements using contingency tables. The sensitivity and specificity statistics, as well as the paired comparison McNemar's test, were calculated using InStat software (GraphPad).

## Results

### Approximal Lesions in Near-IR Images In Vivo

Near-IR imaging was successfully performed on 40 patients *in vivo* with three NIR imaging modalities using custom built optical probes and an InGaAs camera. Figure 2 shows still images captured from a representative approximal lesion acquired using visible light (A), each near-IR modality (B–D), a histological polarized light image (E), and an extra-oral digital radiograph (F). Individual images are extracted frames from real time video captured by the InGaAs camera that was observed by the clinician during the imaging sessions and lesion assessment. The location of the lesion is demarcated by the dashed yellow outline (B–D,F) and the location of the histological cross section (E) is demarcated by the red dashed line in (A). Figure 2B is a near-IR reflectance image acquired at $\lambda$ = 1,500–1,700nm and should be directly compared with visible reflectance (Fig. 2A). When imaging using near-IR reflectance, carious lesions appear bright (white) compared to darker (black) sound enamel, analogous to a white spot lesion. It is clear that there is a marked increase in the contrast of the lesion when imaged using near-IR wavelengths compared to visible light. Figure 2C and D are images acquired from occlusal and approximal near-IR transillumination modalities at $\lambda$ = 1,310nm in which the lesion contrast is flipped relative to the interpretation of near-IR reflectance images. In transillumination sound enamel appears bright (white) and the demineralized tissue appears dark (black). Near-IR occlusal transillumination provides a diagnostic image of the light penetrating upwards to the occlusal surface which can be

attenuated by demineralized enamel regions. In doing so the technique samples the transverse dimensions of the carious lesions which is unique to this modality. Figure 2D is a near-IR approximal transillumination image that should be directly compared with the digital extraoral radiograph shown in Figure 2F in which the lesion appears dark compared to the surrounding sound tissue.

### Occlusal Lesions in Near-IR Images In Vivo

Figure 3 shows a representative sample with occlusal demineralization in the occlusal pits and fissures (A–C) and another sample with staining in the pits and fissures but without decay (D–F). Figure 3A is a visible image of a sample that demonstrates no signs of early demineralization in the pits and fissures even without the presence of stain to mask these early optical changes (clean pits and fissures). Figure 3B is the near-IR cross-polarized reflectance image of the sample which easily identifies decay in the distal pit in high contrast as indicated by the yellow outline. Figure 3C is a PLM image of a histological cross section taken across the pit which reveals the lesion depth to be approaching the dentinoenamel junction. Figure 3D is a visible image of another sample that has stain in the distal pit. Despite the strong absorbance from stain in the visible image, the near-IR cross-polarized reflectance image (Fig. 3E) does not demonstrate any lesion contrast from the distal pit. The histological data from the PLM image (Fig. 3F) confirms that there is no lesion developing in the distal pit of this sample.

### Histological Analysis of Lesion Location and Depth

Transverse microradiography (TMR) performed on 200 μm thick mesiodistal premolar cross sections determined that 105 of 109 (96.3% prevalence) had at least early demineralization (lesion depth ≥E1) on either a proximal or occlusal tooth surface. Carious lesions were more prevalent on the occlusal surface (89/109, 81.7% prevalence) than the mesial or distal proximal surfaces (30/109, 27.5% prevalence) in this premolar population. Thirteen of the 105 (12.4%) carious premolars had coexisting occlusal and proximal lesions. Occlusal and approximal lesions exhibited similar variation in lesion depth determined by a Chi Squared test yielding $\chi^2 = 2.430$ and $P = 0.3$. No severe D2 lesions were found.

### Comparison of Digital Radiographs and Near-IR Imaging

Two clinicians evaluated the extraoral digital radiographs and the near-IR video data acquired during the patient imaging sessions. They carried out the evaluations blinded to the other imaging modalities. The reported diagnoses were stratified by lesion location for each modality and were analyzed for sensitivity and specificity followed by repeated measures McNemar's statistic to test for significance in observed differences between techniques against the histological gold standard, TMR. For carious lesions located on the occlusal tooth surface digital radiographs were only able to identify a single lesion (1/109) and demonstrated a sensitivity of 0.01 (95%CI –0.00 to 0.07) and specificity of 1.00 (95%CI –0.83 to 1.00), (Table 1). The near-IR imaging system demonstrated substantial improvement in the sensitivity to occlusal lesions compared to radiographs yielding a calculated value of 0.49 (95%CI –0.38 to 0.59), and associated specificity of 0.70 (95%CI –0.46 to 1.88). The 95% confidence intervals and McNemar's test show that the near-IR system was more sensitive ($P = 0.0001$) and as specific ($P = 0.077$) as digital radiographs when detecting

occlusal decay. For carious lesions located on proximal tooth surfaces digital radiographs demonstrated a sensitivity of 0.23 (95%CI –0.10 to 0.42) and specificity of 0.96 (95%CI –0.89 to 0.99). The near-IR imaging system demonstrated marked improvement in the sensitivity to detected approximal lesions compared to radiographs yielding a calculated value of 0.53 (95%CI –0.34 to 0.72) and associated specificity of 0.86 (95%CI –0.76 to 0.93). The 95% confidence intervals and McNemar's test show that the near-IR system was more sensitive ($P = 0.013$) and as specific ($P = 0.09$) as digital radiographs when detecting occlusal decay.

### Comparison of the Diagnostic Performance of Individual Near-IR Imaging Probes

The near-IR imaging system employed in this study consisted of three different imaging probes that deliver light into the tooth with different geometries. The sensitivity and specificity of each individual probe for occlusal and proximal surfaces are shown in Table 2. For lesions found on the occlusal surface the near-IR cross-polarized reflectance probe was by far the most sensitive modality measuring 0.48 (95%CI –0.38 to 0.59) with a specificity of 0.70 (95%CI –0.46 to 0.88). For lesions found on the proximal surface each near-IR modality demonstrated similar sensitivity and specificity levels.

## Discussion

In this paper, we present the results from the first clinical study assessing the diagnostic performance of near-IR imaging for screening for dental caries. Teeth were imaged without prior knowledge of lesion presence, whereas in all previous clinical studies, lesions were either previously identified by visual examination or radiography before near-IR imaging.

We anticipated that 10–20% of the premolar teeth would have demineralization in the occlusal grooves and that a sample size of 80–160 teeth would be sufficient, based on our previous study that utilized only teeth with radio-positive lesions on proximal surfaces [4]. Histology indicated that 89 of the 109 teeth had demineralization on the occlusal surfaces and 30 out of the 109 teeth had lesions on the proximal surfaces. The great majority of these lesions were small and confined to the enamel and only 28% penetrated to dentin. It is important to stress that these are small lesions that are much more difficult to detect and image, in comparison to lesions imaged in the recent clinical studies involving the Diagnocam at 780 nm where 96% of the lesions were dentinal lesions [21,22].

The sensitivity of the combined near-IR imaging probes was significantly higher than radiographs for both occlusal and proximal lesions. It was anticipated that near-IR methods would be more sensitive than radiographs since the radiographic sensitivity for occlusal lesions is extremely poor; however, the sensitivity was also much higher for approximal lesions than radiography, 0.53 versus 0.23. In addition, the sensitivity of each near-IR probe was either individually equal to or higher than radiography.

In reflectance, demineralization appears whiter due to increased light scattering by the pores of the lesion and in the near-IR all the lesions appear white because stains do not interfere [3,24]. In transillumination, the lesions appear darker due to light scattering which blocks light from penetrating through the tooth. Water absorption causes sound and demineralized

areas to appear darker both in reflection and transillumination. In reflectance, at wavelengths with higher water absorption (1,600nm and 1,500–1,700nm) absorption by water of the deeply penetrating near-IR causes sound areas of the tooth to appear darker enhancing the contrast.

The greatest surprise of the study was the remarkable performance of near-IR reflectance imaging considering the high absorption of $H_2O$ at the wavelengths employed. It had the highest diagnostic performance of any of the near-IR probes for both occlusal and approximal lesions. Based on our prior studies on extracted teeth, we had anticipated that near-IR reflectance would be extremely sensitive to early demineralization in the pits and fissures of the occlusal surfaces. However, we did not anticipate that near-IR reflectance measurements would pick up approximal lesions located well below the surface, as shown in Figure 2. This is exciting since near-IR reflectance is the easiest method to employ clinically and is potentially the fastest for clinical screening. It only involves shining light on tooth surfaces and does not require careful positioning of the light sources at the contact point in between teeth for approximal transillumination or at the gums for occlusal transillumination. We were initially concerned about the performance of this probe in the clinical environment due to the high absorption of water and the presence of water on tooth surfaces. Air drying for a few seconds was sufficient to maximize the contrast of the lesions and we had more trouble with strong specular reflections from the tooth surface than absorption by water.

Dentists have based their detection of carious lesions on bite-wing radiographs for more than a century and even though such radiographs may not accurately show the depth, activity or cavitation of these lesions, the standard of care has evolved based on such images. Near-IR imaging is a new imaging technology, and it is important to point out that preliminary use of this device by clinicians is needed to develop/evolve methods to effectively interpret the near-IR images in order to assess the depth and severity of the decay and identify potential false positives before this technology can reach its full potential. Only one evaluator was used for each diagnostic technology and that may have had some impact on the statistical outcome. One must also be concerned about over-detection leading to over-treatment by a technology that may be more sensitive than existing methods.

However, since these near-IR devices do not employ ionizing radiation, there are no restrictions on image acquisition and this method is ideal for monitoring lesions over time. In addition, images collected from the multiple probes and imaging geometries can be integrated to produce a more comprehensive picture of the lesion's location. Marked differences of the appearance of stains, composites, and developmental defects such as fluorosis in the near-IR can be exploited to differentiate them from sound enamel and carious lesions.

Near-IR imaging has been shown to be significantly more sensitive ($P < 0.05$) than radiography for the detection of lesions on both occlusal and proximal tooth surfaces *in vivo*. Near-IR imaging methods are ideally suited for screening all tooth surfaces for carious lesions.

## Acknowledgments

The authors acknowledge the support of NIH Grant RO1-DE14698.

Contract grant sponsor: NIH/NIDCR; Contract grant number: R01-DE14698.

## References

1. Fried D, Featherstone JDB, Glena RE, Seka W. The nature of light scattering in dental enamel and dentin at visible and near-IR wavelengths. Appl Optics. 1995; 34(7):1278–1285.
2. Jones, RS., Fried, D. Lasers in Dentistry VIII. Vol. 4610. San Jose: Proc of SPIE; 2002. Attenuation of 1310-nm and 1550-nm laser light through sound dental enamel; p. 187-190.
3. Buhler C, Ngaotheppitak P, Fried D. Imaging of occlusal dental caries (decay) with near-IR light at 1310-nm. Optics Express. 2005; 13(2):573–582. [PubMed: 19488387]
4. Staninec M, Lee C, Darling CL, Fried D. In vivo near-IR imaging of approximal dental decay at 1,310nm. Lasers Surg Med. 2010; 42(4):292–298. [PubMed: 20432277]
5. Darling CL, Huynh GD, Fried D. Light scattering properties of natural and artificially demineralized dental enamel at 1310-nm. J Biomed Optics. 2006; 11(3):034023.
6. Jones, G., Jones, RS., Fried, D. Lasers in Dentistry X. Vol. 5313. San Jose: Proc of SPIE; 2004. Transillumination of interproximal caries lesions with 830-nm light; p. 17-22.
7. Jones RS, Huynh GD, Jones GC, Fried D. Near-IR transillumination at 1310-nm for the imaging of early dental caries. Opt Express. 2003; 11(18):2259–2265. [PubMed: 19466117]
8. Fried D, Featherstone JDB, Darling CL, Jones RS, Ngaotheppitak P, Buehler CM. Early caries Imaging and monitoring with near-IR light. Dent Clin North Am. 2005; 49(4):771–794. [PubMed: 16150316]
9. Hirasuna K, Fried D, Darling CL. Near-IR imaging of developmental defects in dental enamel. J Biomed Opt. 2008; 13(4):044011, 11–17. [PubMed: 19021339]
10. Lee C, Lee D, Darling CL, Fried D. Nondestructive assessment of the severity of occlusal caries lesions with near-infrared imaging at 1310nm. J Biomed Optics. 2010; 15(4):047011.
11. Barenie J, Leske G, Ripa LW. The use of fiber optic transillumination for the detection of proximal caries. Oral Surg. 1973; 36:891–897. [PubMed: 4524840]
12. Pine, CM. Fiber-Optic transillumination (FOTI) in caries diagnosis Early detection of dental caries. Vol. 1996. Indiana University; p. 51-66.
13. Peltola J, Wolf J. Fiber optics transillumination in caries diagnosis. Proc Finn Dent Soc. 1981; 77:240–244. [PubMed: 7267640]
14. Holt RD, Azeevedo MR. Fiber Optic transillumination and radiographs in diagnosis of approximal caries in primary teeth. Community Dent Health. 1989; 6:239–247. [PubMed: 2679987]
15. Mitropoulis CM. The use of fiber optic transillumination in the diagnosis of posterior approximal caries in clinical trials. Caries Res. 1985; 19:379–384. [PubMed: 3861261]
16. Hintze H, Wenzel A, Danielsen B, Nyvad B. Reliability of visual examination, fibre-optic transillumination, and bite-wing radiography, and reproducibility of direct visual examination following tooth separation for the identification of cavitated carious lesions in contacting approximal surfaces. Caries Res. 1998; 32:204–209. [PubMed: 9577986]
17. Schneiderman A, Elbaum M, Schultz T, Keem S, Greenebaum M, Driller J. Assessment of dental caries with digital imaging fiber-Optic transillumination (DIFOTI): In vitro study. Caries Res. 1997; 31:103–110. [PubMed: 9118181]
18. Bin-Shuwaish M, Yaman P, Dennison J, Neiva G. The correlation of DIFOTI to clinical and radiographic images in Class II carious lesions. J Am Dent Assoc. 2008; 139(10):1374–1381. [PubMed: 18832273]
19. Yang J, Dutra V. Utility of radiology, laser fluorescence, and transillumination. Dent Clin North Am. 2005; 49(4):739–752. [PubMed: 16150314]
20. Keem S, Elbaum M. Wavelet representations for monitoring changes in teeth imaged with digital imaging fiber-optic transillumination. IEEE Trans Med Imaging. 1997; 16(5):653–663. [PubMed: 9368121]

21. Kuhnisch J, Sochtig F, Pitchika V, Laubender R, Neuhaus KW, Lussi A, Hickel R. In vivo validation of near-infrared light transillumination for interproximal dentin caries detection. Clin Oral Investig. 2015; 20(4):821–829.
22. Sochtig F, Hickel R, Kuhnisch J. Caries detection and diagnostics with near-infrared light transillumination: Clinical experiences. Quintessence Int. 2014; 45(6):531–538. [PubMed: 24618570]
23. Karlsson L, Maia AMA, Kyotoku BBC, Tranaeus S, Gomes ASL, Margulis W. Near-infrared transillumination of teeth: Measurement of a system performance. J Biomed Optics. 2010; 15(3): 036001.
24. Zakian C, Pretty I, Ellwood R. Near-infrared hyperspectral imaging of teeth for dental caries detection. J Biomed Optics. 2009; 14(6):064047.
25. Almaz, EC., Simon, JC., Fried, D., Darling, CL. Lasers in Dentistry XXII. Vol. 9692. San Francisco: Proc of SPIE; 2016. Influence of stains on lesion contrast in the pits and fissures of tooth occlusal surfaces from 800-01600-nm; p. 1-6.
26. Chung S, Fried D, Staninec M, Darling CL. Multispectral near-IR reflectance and transillumination imaging of teeth. Biomed Opt Express. 2011; 2(10):2804–2814. [PubMed: 22025986]
27. Chong SL, Darling CL, Fried D. Nondestructive measurement of the inhibition of demineralization on smooth surfaces using polarization-sensitive optical coherence tomography. Lasers Surg Med. 2007; 39(5):422–427. [PubMed: 17565731]
28. Wu J, Fried D. High contrast near-infrared polarized reflectance images of demineralization on tooth buccal and occlusal surfaces at lambda=1310-nm. Lasers Surg Med. 2009; 41(3):208–213. [PubMed: 19291753]
29. Fried, D., Staninec, M., Darling, CL., Kang, H., Chan, K. Lasers in Dentistry XVII. Vol. 7884. San Jose: Proc of SPIE; 2011. In vivo near-IR imaging of occlusal lesions at 1310-nm; p. 1-7.
30. Fried WA, Darling CL, Chan K, Fried D. High contrast reflectance imaging of simulated lesions on tooth occlusal surfaces at near-IR wavelengths. Lasers Surg Med. 2013; 45:533–541. [PubMed: 23857066]
31. Simon JC, Chan KH, Darling CL, Fried D. Multispectral near-IR reflectance imaging of simulated early occlusal lesions: Variation of lesion contrast with lesion depth and severity. Lasers Surg Med. 2014; 46(3):203–215. [PubMed: 24375543]
32. Staninec M, Douglas SM, Darling CL, Chan K, Kang H, Lee RC, Fried D. Nondestructive clinical assessment of occlusal caries lesions using near-IR imaging methods. Lasers Surg Med. 2011; 43(10):951–959. [PubMed: 22109697]
33. Peers A, Hill FJ, Mitropoulos CM, Holloway PJ. Validity and reproducibility of clinical examination, fibre-optic transillumination, and bite-wing radiology for the diagnossis of small approximal carious lesions. Caries Res. 1993; 27:307–311. [PubMed: 8402807]
34. Pine CM, ten Bosch JJ. Dynamics of and diagnostic methods for detecting small carious lesions. Caries Res. 1996; 30(6):381–388. [PubMed: 8946093]
35. Purdell-Lewis DJ, Pot T. A comparison of radiographic and fibre-optic diagnoses of approximal caries lesions. J Dent. 1974; 2(4):143–148. [PubMed: 4531441]
36. Vaarkamp J, ten Bosch JJ, Verdonschot EH, Bronkhoorst EM. The real performance of bitewing radiography and fiberoptic transillumination in approximal caries diagnosis. J Dent Res. 2000; 79(10):1747–1751. [PubMed: 11077989]
37. Stephen KW, Russell JI, Creanor SL, Burchell CK. Comparison of fibre optic transillumination with clinical and radiographic caries diagnosis. Community Dent Oral Epidemiol. 1987; 15(2):90–94. [PubMed: 3552397]
38. Darling, CL., Featherstone, JDB., Le, CQ., Fried, D. Lasers in Dentistry VX. Vol. 7162. San Jose: Proc of SPIE; 2009. An automated digital microradiography system for assessing tooth demineralization; p. 1-7.

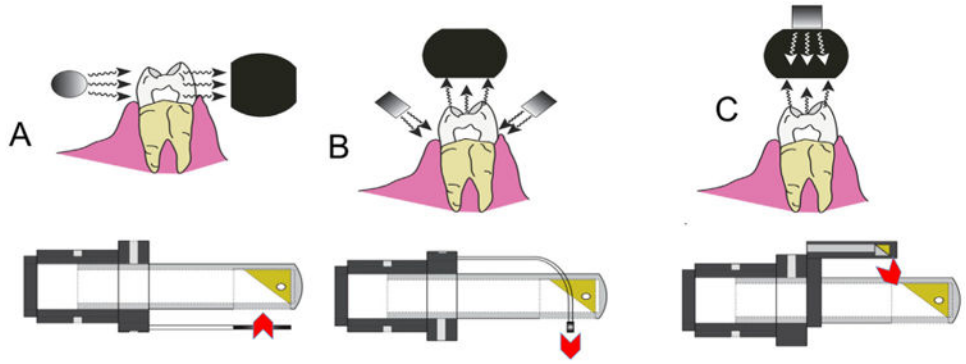


**Fig. 1.**

Imaging configurations and diagrams for the three near-IR imaging probes used in the study. (**A**) Near-IR approximal transillumination at 1,310 nm, (**B**) near-IR occlusal transillumination at 1,310nm and (**C**) cross-polarized near-IR reflectance at 1,500–1,700nm. On the upper diagrams the arrows pointing towards the tooth show the position of illumination while the arrows pointing away from the tooth show the reflected or transmitted light incident on the camera. On the lower diagrams the camera is attached to the left side of each probe, the red arrows show the direction of the light emanating from each probe, and the reflecting prisms are shown in yellow.

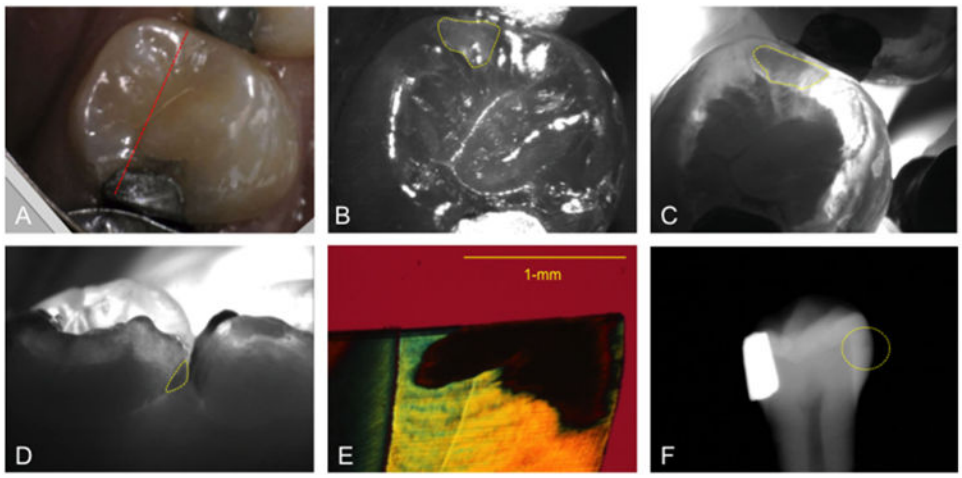


**Fig. 2.**

Images of an approximal lesion located 2–3mm below the occlusal surface. Visible light (**A**), near-IR reflectance (**B**), near-IR occlusal transillumination (**C**), near-IR approximal transillumination (**D**), histological polarized light image (**E**), and extra-oral digital radiograph (**F**). Dashed yellow margin outlines the lesion areas. The dashed red line in (**A**) indicates location of histological sample slice in (**E**).

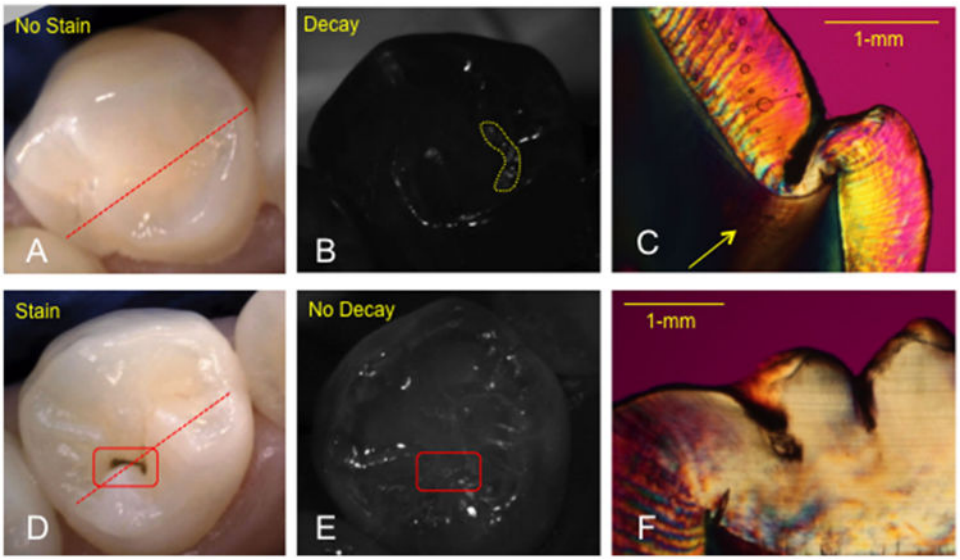


**Fig. 3.**

Images of an unstained fissure with demineralization (**A–C**). Visible light (**A**), near-IR reflectance (**B**), and histological polarized light image (**C**). Images of a stained fissure without demineralization (**D–F**). Visible light (**D**), near-IR reflectance (**E**), and histological polarized light image (**F**). The yellow dashed margin in (**B**) indicates lesion areas and the red dashed box in (D and **E**) shows the position of the stained fissue. The dashed red lines in (**A** and **D**) indicate the location of histological sample slices in (**C** and **F**). The yellow arrow in (**C**) points to the dentin affected by the lesion in the fissure.

## Table 1

**Sensitivity and Specificity Calculations for Digital Radiographs and the NIR Imaging System Stratified by Lesion Location Compared to the Gold Standard TMR Histology**

| | Diagnostic performance | | | |
|---|---|---|---|---|
| | Occlusal | | Proximal | |
| Diagnostic variable | X-ray | NIR | X-ray | NIR |
| Sensitivity | 0.01 | 0.49 * | 0.23 | 0.53 * |
| (95%CI) | (0.00–0.07) | (0.38–0.59) | (0.10–0.42) | (0.34–0.72) |
| Specificity | 1.00 | 0.70 | 0.96 | 0.86 |
| (95%CI) | (0.83–1.00) | (0.46–0.88) | (0.89–0.99) | (0.76–0.93) |

McNemar's test and 95% confidence intervals were used to determine the significance of the results.

* Indicates statistical significance between digital radiographs and the NIR imaging system.

**Table 2**

**Sensitivity and Specificity Calculations for Each NIR Imaging Probe Stratified by Lesion Location Compared to the Gold Standard TMR Histology**

| | Individual NIR probe diagnostic performance | | | | | |
|---|---|---|---|---|---|---|
| | Occlusal | | | Proximal | | |
| Diagnostic variable | R | O | P | R | O | P |
| Sensitivity | 0.48 | 0.08 | – | 0.27 | 0.23 | 0.23 |
| (95%CI) | (0.38–0.59) | (0.03–0.16) | | (0.12–0.46) | (0.1–0.42) | (0.10–0.42) |
| Specificity | 0.70 | 0.95 | – | 0.92 | 0.91 | 0.96 |
| (95%CI) | (0.46–0.88) | (0.75–1.00) | | (0.84–0.97) | (0.83–0.96) | (0.89–0.99) |

R, reflectance; O, occlusal transillumination; P, approximal transillumination.
95% confidence intervals were used to determine the significance of the results.